

Kinetics of Ceramic Phase Crystallization in a Glass Derived from Wastes of Iron and Steel Industry

S. Ghasemi ^{*1}, A. Shafyei ²

¹ Department of Metallurgy and Materials Engineering, Hamedan University of Technology, Hamedan, 65155-579, Iran

² Department of Materials Engineering, Isfahan University of Technology, Isfahan, 8415683111, Iran

Abstract

Intensified environmental regulations have posed numerous challenges in the disposal of industrial wastes. The steel industry is one of the biggest production industries, with a considerable amount of daily wastes. Production of glass-ceramic from the steel industry wastes is one of the proper solutions for this problem. In this study, the utilization of different wastes (such as blast-furnace slag, converter slag and dust) as the raw material for glass-ceramic production was evaluated. After mixing the precursors, the mixture was melted at 1450. The obtained melt was cooled down at cooling rate of 10°C/min in metallic molds, and the glass was derived. Ceramic phases were grown by application of isothermal heat treatment periods up-to 6 h, at 750, 800, 850, and 900. The mean length of the ceramic phases was measured after each heat treatment period by scanning electron microscopy. It was shown that crystal growth followed a parabolic kinetic model. The activation energy of crystallization was also determined as 129 kJ/mol in the temperature range of 750-900°C.

Keywords: Steel making; Wastes; Glass-Ceramics; Crystallization; Kinetics.

1. Introduction

Glass-ceramic materials are polycrystalline solids obtained through melting of the raw materials and their molding in the form of a glass followed by heat treatment to induce ceramic phase crystallization. During the crystallization, the nucleation and growth of ceramic

crystals occurs from the main glass phase. The number of crystals, their growth rate, and therefore, their final grain size can be controlled by the proper heat treatment. After crystallization, some glass phase always remains in the structure as the matrix. Glass-ceramics possess the properties of glasses and ceramics simultaneously ¹⁾.

Various precursors can be used in the production of glass-ceramics, which will result in a wide range of chemical compositions and hence, different properties. Like any other production process, the price of precursors can significantly affect the final cost of the glass-ceramics. The use of inexpensive precursors such as basalts ^{2,3)}, as well as waste materials such as metallurgic slags ⁴⁻⁹⁾, using steel industry slags and power plant waste ¹⁰⁾, fly ash 11–15 appropriate management and treatment of the residues have become an urgent environmental protection problem. This work investigated the preparation of a glass-ceramic from a mixture of bottom ash and fly

* Corresponding author

Email: samad.ghasemi@hut.ac.ir

Tell: +98 813 8411460

Address: Department of Metallurgy and Materials Engineering, Hamedan University of Technology, Hamedan, 65155-579, Iran

1. Assistant Professor

2. Professor

ash by peturgic method. The nucleation and crystallization kinetics of the new glass-ceramic can be obtained by melting the mixture of 80% bottom ash and 20% fly ash at 950°C, which was then cooled in the furnace for 1h. Major minerals forming in the glass-ceramics mainly are gehlenite ($\text{Ca}_2\text{Al}_2\text{SiO}_7$), hydrometallurgical zinc extraction wastes¹⁶⁾ and electric arc furnace dust^{17,18)} can dramatically reduce the production cost of glass-ceramics. In addition to reducing the production costs, the re-use of these materials can resolve their environmental problems.

Crystallization refers to a process by which a regular network of crystals will be formed from a melt or glassy solid¹⁾. The process of producing glass-ceramic from the raw glassy article includes two stages: nucleation and growth of the ceramic phase. In this research, the initial glass was fabricated by melting the wastes of an iron and steel factory, followed by its rapid cooling. The details of the nucleation stage and crystallization mechanism were discussed in the previous paper¹⁹⁾. The crystallization kinetics of waste derived glass-ceramics have been investigated by several researchers²⁰⁻²⁴⁾. As the chemical composition of waste-derived glass ceramics is complicated, its crystallization behavior and kinetics will be not the same for different glass compositions. This study is

aimed to investigate the kinetics of the crystallization and the growth rate of the ceramic phases in this glass.

2. Materials and Methods

In this study, Mixtures of iron and steel making wastes of a steel plant were used as raw materials. The 10 kg charge mixture was prepared for melting using 18% blast furnace slag, 9% blast furnace dust, 5% converter slag, 12% converter sludge, 7% agglomeration sludge, 30% silica sand, 12% fluorine and 7% sodium carbonate. The chemical composition of raw materials was determined by X-ray fluorescence (XRF, Bruker, S4pioneer, Germany), and the results are presented in Table. 1. According to Table 1, the major components of the blast furnace slag are SiO_2 and CaO. In contrast, for blast furnace dust, converter sludge and agglomeration sludge, the major components are iron oxides. Also, there is a vast amount of residual carbon in the composition of blast furnace dust, and agglomeration sludge. Silica sand was added to improve glass formation ability during cooling of glass melt. Fluorine and sodium carbonate were added as fluxes to decrease the melting temperature and making the glass melt homogeneous.

Table. 1. Chemical composition (wt. %) of raw materials.

	SiO_2	CaO	MgO	Al_2O_3	FeO	Fe_2O_3	TiO_2	K_2O	Na_2O	L.O.I
Blast Furnace Slag	36.4	35.41	8.85	9.6	1.11	0	3.14	0.81	0.4	0
Blast Furnace Dust	10	5.36	1.81	1.86	10.5	36.37	0	0.42	0.31	32
Converter Slag	14.6	45.22	4.85	3.92	7.41	12	1.08	0.11	0.31	0
Converter Sludge	1.53	6.3	1.7	0.65	11.8	71.21	0.28	0.52	0.27	3.5
Agglomeration Sludge	10.41	12.23	3.76	3.06	5.8	28.66	0.78	0.45	0.27	30.4

The raw materials batch was melted in a silicon carbide crucible at 1400C for 1 hr in an oil fuel-fired furnace. To have more homogeneity, the melt was stirred mechanically every 10 minutes during melting. The resultant glass melt was poured in $1 \times 2 \times 5$ cm³ steel molds (preheated at 400 °C). The samples then immediately were transferred to a 500C electric furnace to avoid thermal shocks. After 1 hr annealing at 500°C, the samples were cooled down to room temperature in the furnace.

The X-ray diffraction (XRD) method was used to reveal the crystalline phase(s) formed during heat treatment. An XL-30 Philips diffractometer (40 kV) with Cu-K α radiation was used for XRD measurements. The microstructure of glass and glass-ceramic samples was investigated by a Philips XL30 scanning electron microscopy, equipped with EDS. To get good contrast in SEM investigations, the samples were etched in 5% HF acid for 10 s and then coated with a thin gold film. The mi-

cro-hardness of each phase was determined by a Vickers' indenter at 200 g load and dwell time of 15 s. Ten indentations were made on each sample to obtain an average value of hardness. The three-point flexural strength of the glass and glass ceramics were also measured at room temperature by using specimens according to ASTM C158 at a cross-head speed of 2 mm/min.

For analysis of ceramic crystallization kinetics, it must be noted that the growth rate at each temperature (V) can be obtained from the slope of the plot of the ceramic phase size versus the time^{25, 26)}.

$$V = \frac{\Delta x}{\Delta t} \quad (1)$$

$$V = V_0 e^{-\frac{Q}{RT}} \quad (2)$$

$$\ln(V) = \ln(V_0) - \frac{Q}{RT} \quad (3)$$

Thus by plotting $\ln(V)$ as a function of $1/T$, a straight line will be obtained whose slope is $-Q/R$. Activation energy is a crucial kinetic parameter, which can be calculated by this method.

3. Results and Discussions

Table. 2 shows the chemical analysis of the raw materials mixture before melting and the chemical composition of the as-cast glass (after melting). It can be seen

Table. 2. Chemical composition (wt. %) of the employed formulation before and after melting.

Composition (%)	SiO ₂	CaO	MgO	Al ₂ O ₃	FeO	Fe ₂ O ₃	TiO ₂	K ₂ O	Na ₂ O	CaF ₂	LOI
Before melting	51.49	10.50	1.40	1.08	3.37	12.41	0.28	0.11	4.20	10	4.92
After melting	53.2	12.1	3.4	3.08	10.53	0.96	1.5	0.35	4.2	10.3	0

As mentioned in our previous study¹⁹, diopside phase is crystallized on iron micro-particles during crystallization of the steel waste derived glass. These iron micro-particles are produced in-situ and dispersed in the glass melt as a result of reduction of iron oxides with carbon presented in the raw materials. As a result of the presence of such metallic iron micro particles, ceramic phases with diameter less than 10 μm is produced. During heat treatment, the ceramic phases started to grow

from this table that some compositional changes occurred after melting, especially, decreasing the total content of iron oxides. It indicates a relative increasing in the $\text{Fe}^{+2}/\text{Fe}^{+3}$ ratios in as-cast glass, compared to that ratio in the batch before melting. Also, some iron was reduced to metallic iron and settled at the bottom of the crucible as iron melted. The increased $\text{Fe}^{+2}/\text{Fe}^{+3}$ ratio and complete reduction of some iron oxides can be explained through the reduction reaction between iron oxides and residual carbon in raw materials.

gradually. The mean length of the crystallized ceramic phases at different times and heat treatment temperatures are provided in Table 3. The length of the ceramic phases was measured by SEM micrography.

Kinetic investigation of the growth of ceramic phases in glass-ceramics reported by some researchers has shown that the growth rate has an exponential relationship with the inverse of time.

Table. 3. The mean length of the ceramic phases formed at different times and various heat treatment temperatures.

700°C		750°C		800°C		850°C	
Time (min)	D (μm)	Time (min)	D (μm)	Time (min)	D (μm)	Time (min)	D (μm)
0	0	0	0	0	0	0	0
120	1.88	60	2.19	60	2.80	60	3.44
240	2.19	120	3.13	120	4.06	120	5.31
345	2.80	285	4.38	240	5.63	285	7.19

The results of applying Eqs. (1-3) on the kinetic data of this study are presented in Fig. 1. As can be seen, the experimental data are highly scattered in a way that no

straight line can be fitted to them. So, Eqs. (1-3) are not suitable for describing the kinetics of the crystals growth in the studied system.

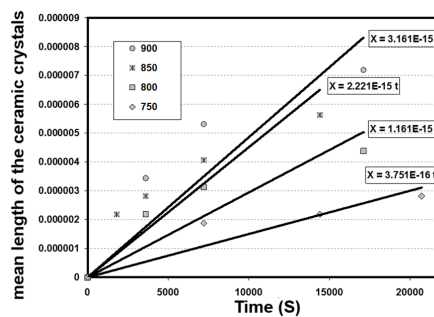


Fig. 1. Fitting a linear relationship for the mean length of the ceramic grains and time.

Eq. (1) can be used for systems in which the growth of the second phase does not require the elemental diffusion from long distances to the interface, in such conditions; the rate-controlling step is the jumping of atoms from the interface and their linkage to the growing phase. Under such a situation, growth has a constant rate, and the length of the forming phase has a linear relationship with time. This condition occurs in systems whose the chemical composition of primary phase and secondary grown phase are similar together²⁵.

In this study, as the precursors were low purity wastes with lots of oxide materials, it was impossible to create a final composition similar to the stoichiometric composition of the diopside ceramic phase (Ca(Fe,Mg)

Si₂O₆) Therefore, some oxides should be repelled while some others must be transferred to the ceramic phase. Thus, the growth process can be considered as a diffusion-controlled process. Fig. 2 presents the difference in the chemical composition of the growing ceramic phase and that of the background phase (glass) determined by microanalysis. For instance, Si and Ca were repelled to the residual glass phase while Fe and Mg accumulated in the ceramic phase. As the crystallization is a solid state process, the mass transport mechanism is solid state diffusion as well. The equations regarding the growth of the secondary phase and their fitting with the experimental results were assessed.

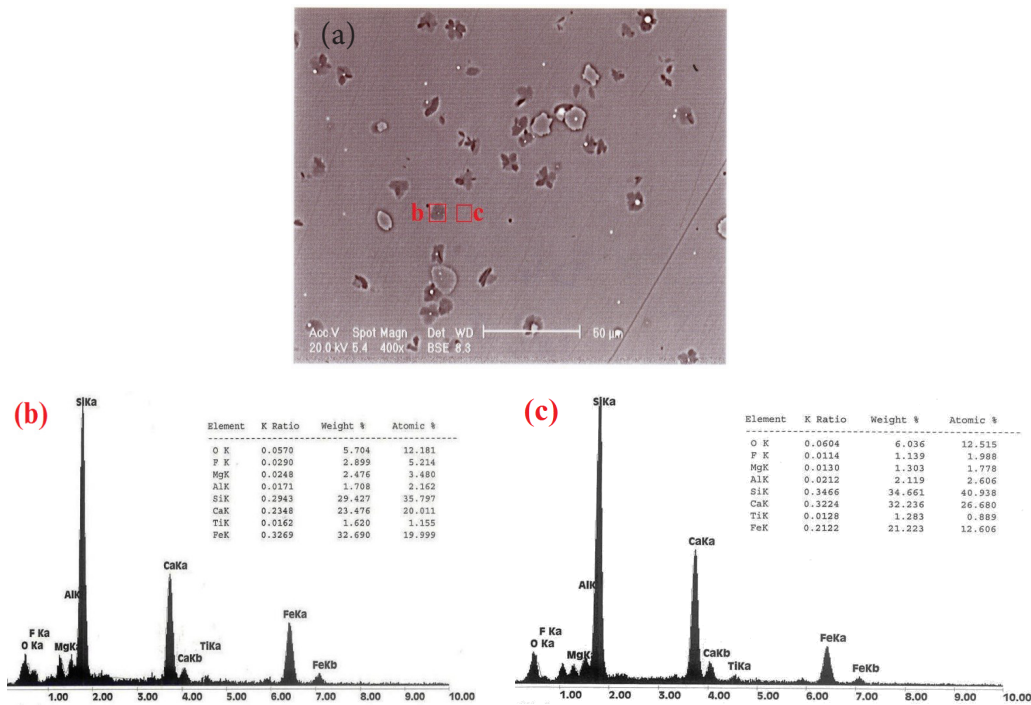


Fig. 2. a) Microstructure of glass-ceramic after partial crystallization at 800°C. In this Fig., *b* denoted the ceramic particle and *c* is the glass Matrix. b) EDS analysis of the ceramic crystals, and c) EDS analysis of the residual glass matrix.

Consider a ceramic-glass interface in which the growing ceramic phase is richer in one of the elements (compared to the glass matrix); let V be the growth rate²⁷. As the concentration of the intended composition is higher in the ceramic phase (C_β) compared to the matrix (C_0), the glass matrix will be poor in the intended element in the vicinity of the interface. A local equilibrium can be considered in the glass-ceramic interface. This local equilibrium means that the concentration of the intended composition in the matrix (at the vicinity of the ceramic phase) is equal to an equilibrium level (C_e). At this condition, the growth rate will depend on the concentration gradient at the interface (dC/dx). For the unit area of the interface to grow by dx , a volume of $V \times dx$ from the glass phase with the composition of C_e should be converted

to the ceramic phase with the composition of C_β . This discussion implies that $(C_\beta - C_e) \cdot dx$ moles of element β should reach the interface from the regions far from the interface. Therefore, the flux of β per unit area in dt will be $D \cdot (dC/dx) \cdot dt$. In which D shows the diffusion coefficient of β in the glass matrix. Combining these two equations we have:

$$v = \frac{dx}{dt} = \frac{D}{C_\beta - C_e} \cdot \frac{dC}{dx} \quad (4)$$

Within this time, the ceramic phase composition (C_β) should reach itself from long distances to the interface. Therefore, the chemical composition gradient at the interface, dC/dx , will be reduced by time. To simplify the

equations, suppose that the concentration gradient varies linearly in the interface. Thus, dC/dx will be $\Delta C_0/L$ in which $\Delta C_0=C_0-C_e$ and L denotes the diffusion distance. According to the mass conservation principle:

$$(C_\beta - C_0).x = L.\Delta C_0/2 \quad (5)$$

In the above equation, x shows the thickness of the ceramic phase. The growth equation can be written as:

$$v = \frac{D(\Delta C_0)^2}{2(C_\beta - C_e)(C_\beta - C_0)x} \quad (6)$$

Considering a constant molar volume (V_m), the concentrations can be replaced by the molar fraction ($X=C.Vm$). Moreover, it can be regarded that $C_\beta - C_0 \approx C_\beta - C_e$ which may simplify the equations. By integrating from Eq. (6):

$$x = \frac{\Delta X_0}{\sqrt{(X_\beta - X_e)}} \cdot \sqrt{(Dt)} \quad (7)$$

$$v = \frac{\Delta X_0}{2.(X_\beta - X_e)} \cdot \sqrt{\left(\frac{D}{t}\right)} \quad (8)$$

In which $\Delta X_0 = X_0 - X_e$ is equal to the super-saturation in the glass phase.

Considering the mentioned equations, the following points can be drawn:

1- The ceramic phase growth follows the parabolic growth principle:

$$x \propto \sqrt{(Dt)} \quad (9)$$

$$v \propto \sqrt{\left(\frac{D}{t}\right)} \quad (10)$$

Such behavior and its governing equations can be well observed in the crystallization of some of the glass systems²⁸.

Figure 2 shows the impact of glass chemical composition and temperature on the growth rate of the ceramic phase. At high temperatures (low cooling), the growth rate is low. Due to lower super-saturation (ΔX_0), the growth rate also declines in the low temperatures as a result of a reduction in the diffusion rate. Regarding the contradicting effect of these two parameters (diffusion coefficient and super-saturation), the maximum growth rate occurs in intermediate temperatures. For the studied glass-ceramic system, the impact of temperature is more profound on the diffusion; thus, a descending pattern can be observed in the growth rate by temperature reduction.

Eq. (8) is applicable in the cases where the diffusion zones of growing phases do not interfere with each other²⁷. Under such conditions, the growth rate will be declined very rapidly and finally stop when the composition of the residual glass throughout the zones reaches X_e . Using Eq. (7):

$$x^2 = \left(\frac{\Delta X_0}{\sqrt{(X_\beta - X_e)}}\right)^2 \cdot (Dt) \quad (11)$$

Considering $A = \frac{\Delta X_0}{\sqrt{(X_\beta - X_e)}} :$

$$x^2 = A.(Dt) \quad (12)$$

It can be seen that the square of the grains' mean length is linearly related to the time at a constant temperature. The slope of the line is $A.D$, which is proportional to D . These equations were fitted with the kinetic results of ceramic phase growth in a glass investigated in this research, Fig. 3, which shows right consistency.

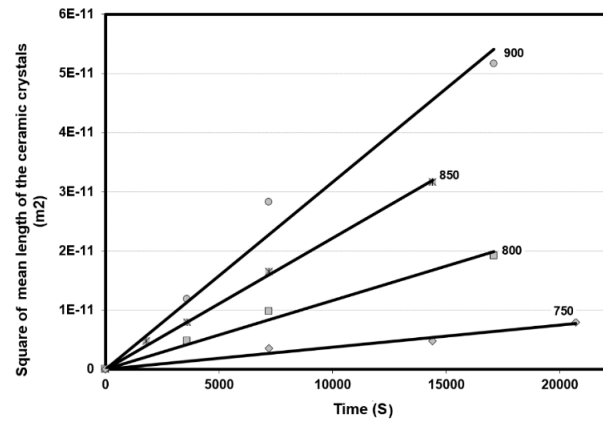


Fig. 3. Square of ceramic crystals lengths versus time at various isothermal crystallization temperatures.

As the diffusion coefficient exponentially varies by temperature:

$$A.D = A_0.D_0.e^{-\frac{Q}{RT}} \quad (13)$$

Substituting Eq. (13) in Eq. (12):

$$\ln(A.D) = \ln(A_0.D_0) - \frac{Q}{RT} \quad (14)$$

The slope of the lines plotted in Fig. 3 is proportional to the diffusion coefficients at the same temperature. Thus by their application in Eq. (14) and plotting $\ln(A.D)$ versus $1/T$ (Fig. 8), a straight line will be obtained with the slope of -1553. This value is equal to $-Q/R$. As $R=8.314$ J/(mol.K), the growth activation energy (Q) will be obtained as 129 kJ/mol. Overall growth equation can be written as:

$$x = \sqrt{(3.77 \times 10^{-9} \cdot e^{\left(\frac{-15533}{T}\right)})t} \quad (15)$$

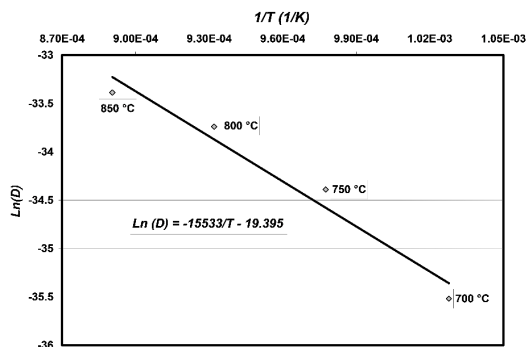


Fig. 4. Determination of activation energy and the growth equation for the growth of ceramic phases in the glass matrix.

Previous studies on the crystallization of $\text{MgO-Al}_2\text{O}_3\text{-SiO}_2$ glass showed high activation energy, 433 kJ/mol²⁹⁾. Such high activation energy can be attributed to the high purity of the base glass, and hence, its high melting point and high diffusion coefficient. The high activation energy in the $\text{Fe}_2\text{O}_3\text{-CaO-SiO}_2$ system was also high, 636 kJ/mol, due to same reasons. This system was prepared from pure precursors. In a glass with a relatively similar composition, which was prepared from low-purity wastes plus Na_2O (as melting flux), activation energy was drastically reduced from 636 to 377 kJ/mol³¹⁾. Therefore, the lower activation energy of crystallization in this research is at-

tributed to the lower purity of base glass, which resulted in the diffusion at lower activation energies.

Fig. 5 shows the XRD pattern of the base glass, after heat treatment of glass at 700°C for nucleation of ceramic phases and after heat treatment at 850°C for growth of ceramic phases. The pattern reveals the amorphous base glass. The diffraction pattern of nucleated sample is almost similar to the base glass, indicating that no ceramic phase was grown during nucleation treatment at 700°C. After heating for 1 hr at 850 °C, the diopside phase, $\text{Ca(Fe,Mg)Si}_2\text{O}_6$, was crystallized as the main ceramic phase.

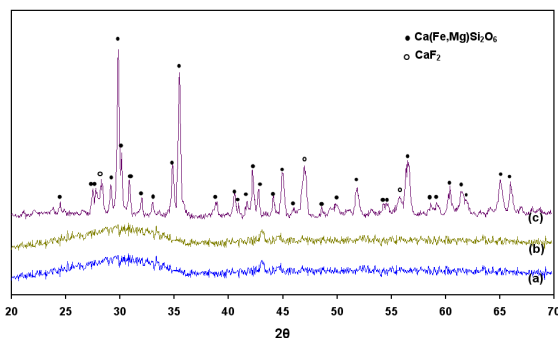


Fig. 5. XRD pattern of (a) base glass, (b) nucleation heat treatment at 700°C for 1 hr and (c) growth heat treatment of ceramic phases at 850 °C for 1 hr.

The results of flexural strength and micro hardness of base glass, nucleated and crystallized glass is presented in Table 4. The crystallization of the glass improves bending strength, while it has no considerable effect on Vickers micro hardness. Crystallization produces a material having greater flexural strength compared to the initial glass. The flexural strength of base glass was 52.7 ± 5

MPa, while the crystallized sample showed a flexural strength of 88.3 ± 5 MPa. It can be concluded that the improvement of flexural strength by incorporating ceramic particles may be attributed to the homogeneous distribution of the ceramic phase in the matrix which prevents the crack propagation in the glass ceramic material¹⁾.

Table 4. Mechanical properties of the base glass and glass-ceramics.

	Vickers microhardness	Flexural Strength (MPa)	Density (gr/cm ³)
Base Glass	753±18	52.7±5	2.57±0.02
Heat treated 1hr at 700°C	768±21	59.2±5	2.63±0.02
Heat treated 1hr at 850°C	824±21	88.3±5	2.74±0.02

4. Conclusions

Microstructural investigations and EDS elemental analysis revealed elemental partitioning between the growing ceramic phase and the residual glass. Fe and Mg diffused to the ceramic phase, while Ca and Si were repelled to the glass phase. This partitioning could be attributed to the dissimilarity of the initial glass composition with the chemical composition of the diopside ceramic phase. Kinetic investigations of isotherm crystallization showed that the ceramic phase growth followed a parabolic pattern. The activation energy was 129 kJ/mol. Such a relatively low activation energy (compared to glass-ceramics prepared from high-quality precursors) can be attributed to the impurity of the glass used in this study which resulted in diffusion at lower activation energies.

References

- [1] G. S. Upadhyaya, W. Holland, G. Beall: *Sci. Sinter.*, (2004). 215
- [2] G. A. Khater, A. Abdel-Motelib, A. W. El Manawi, M. O. Abu Safiah: *J. Non. Cryst. Solids.* 358(2012), 1128.
- [3] M. Pavlovic: *Materials (Basel).*, 12(2019).
- [4] V. Gomes, C. D. G. De Borba, H. G. Riella: *J. Mater. Sci.*, 37(2002), 2581.
- [5] R. D. Rawlings, J. P. Wu, A. R. Boccaccini: *J. Mater. Sci.*, 41(2006), 733.
- [6] A. Kamusheva, E. M. A. Hamzawy, A. Karamanov: *J. Chem. Techn. Metal.*, 50(2015).
- [7] M. W. Choi, S. M. Jung: *melt. Iron.mak. Steel.mak.*, 45(2018), 441.
- [8] D. Shin et al.: *Sci. Adv. Mater.*, 8(2016), 2295.
- [9] A. A. Francis: *J. Eur. Ceram. Soc.*, 24(2004), 2819.
- [10] G. S. Back, H. S. Park, S. M. Seo, W. G. Jung: *Met. Mater. Int.*, 21(2015), 1061.
- [11] D. H. Vu, K. S. Wang, J. H. Chen, B. X. Nam, B. H. Bac, *Waste Manag.*, 32(2012), 2306.
- [12] M. Sutcu, et al.: *J. Clean. Prod.* 233(2019), 753.
- [13] C. Leroy, M. C. Ferro, R. C. C. Monteiro, M. H. V. Fernandes: *J. Eur. Ceram. Soc.*, 21(2001), 195.
- [14] M. Erol, S. Küçükbayrak, A. Ersoy-Meriçboyu, M. L. Öveçollu: *J. Eur. Ceram. Soc.*, 21(2001), 2835.
- [15] T. W. Cheng, Y. S. Chen: *Ceram. Int.* 30(2004), 343.
- [16] M. Pelino: *Glass ceramic materials. Waste Manag.* 20 (2000), 561.
- [17] M. Pelino, A. Karamanov, P. Pisciella, S. Crisucci, D. Zonetti: *Waste Manag.* 22(2002), 945.
- [18] A. Nazari, A. Shafyeyi, A. Saidi: *Mater. Chem. Phys.* 205(2018), 436.
- [19] S. Ghasemi, A. Shafyeyi: *Int. J. Iron Steel Soc. Iran.* 14 (2017), 17.
- [20] Z. Lu, J. Lu, X. Li, G. Sha: *Ceram. Int.* 42 (2016), 3452.
- [21] J. Shi, F. He, J. Xie, X. Liu, H. Yang: *J. Non. Cryst. Solids* 491(2018), 106.
- [22] C. Başaran, N. Canikoğlu, H. Özkan Toplan, N. Toplan: *J. Therm. Anal. Calorim.* 125(2016), 695.
- [23] Z. Bai, G. Qiu, C. Yue, M. Guo, M. Zhang: *Ceram. Int.* 42(2016), 19329.
- [24] J. McCloy, et al. Final report: Understanding influence of thermal history and glass chemistry on. (2018). doi: 10.2172/1485494.
- [25] D. Švadlák, P. Pustková, P. Košťál, J. Málek: *Crystal growth kinetics in (GeS₂)_{0.2}(Sb₂S₃)_{0.8} glass. Thermochim. Acta* 446(2006), 121.
- [26] J. Málek, D. Švadlák, T. Mitsuhashi, H. Haneda: *J. Non. Cryst. Solids* 352(2006), 2243.
- [27] D. A. Porter, K. E. Easterling: *Phase transformation. metals and alloys.* (Chapman and Hall, 1982).
- [28] R. G. Duan, K. M. Liang, S. R. Gu: *Mater. Res. Bull.* 33(1998), 1143.
- [29] H. Shao, K. Liang, F. Peng: *Ceram. Int.* 30(2004), 927.
- [30] Y. K. Lee, & S. Y. Choi: *J. Mater. Sci.* 32(1997), 431.
- [31] A. Karamanov, C. Cantalini, M. Pelino, A. Hreglich: *J. Eur. Ceram. Soc.* 19(1999), 527.